Provided for non-commercial research and education use.
Not for reproduction, distribution or commercial use.

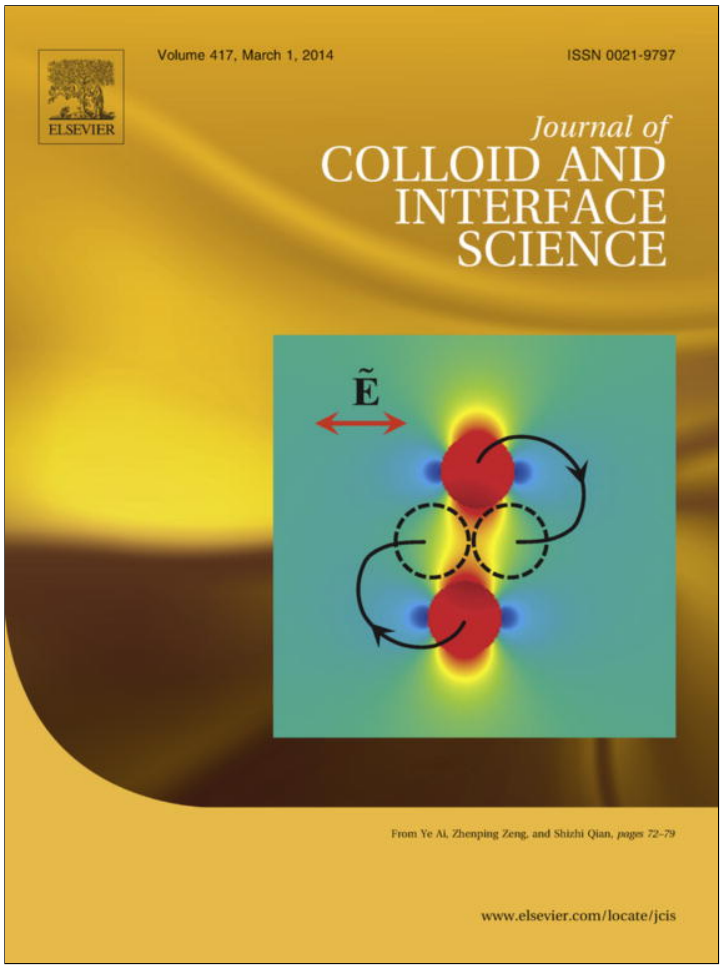


This article appeared in a journal published by Elsevier. The attached copy is furnished to the author for internal non-commercial research and education use, including for instruction at the authors institution and sharing with colleagues.

Other uses, including reproduction and distribution, or selling or licensing copies, or posting to personal, institutional or third party websites are prohibited.

In most cases authors are permitted to post their version of the article (e.g. in Word or Tex form) to their personal website or institutional repository. Authors requiring further information regarding Elsevier's archiving and manuscript policies are encouraged to visit:

http://www.elsevier.com/authorsrights

Author's personal copy

Journal of Colloid and Interface Science 417 (2014) 244–249

Contents lists available at ScienceDirect

Journal of Colloid and Interface Science

www.elsevier.com/locate/jcis

# Effects of nanoparticle size and charge on interactions with self-assembled collagen

Dongbo Wang [a], Jing Ye [a], Steven D. Hudson [b], Keana C.K. Scott [c], Sheng Lin-Gibson [a,*]

[a] Biosystems and Biomaterials Division, National Institute of Standards and Technology, 100 Bureau Drive, Gaithersburg, MD, 20899, USA
[b] Materials Science and Engineering Division, National Institute of Standards and Technology, 100 Bureau Drive, Gaithersburg, MD, 20899, USA
[c] Materials Measurement Science Division, National Institute of Standards and Technology, 100 Bureau Drive, Gaithersburg, MD, 20899, USA

ARTICLE INFO

*Article history:*
Received 29 August 2013
Accepted 8 November 2013
Available online 20 November 2013

*Keywords:*
Adsorption
QCM-D
Toxicity
Biomineralization

ABSTRACT

*Hypothesis:* Insights into bone formation have suggested that the critical first step in the biomineralization process is the integration of small (nanometer dimension) mineral clusters into collagen fibers. Not only is such behavior of interest for understanding biomineralization but also should be important to nanotoxicology because collagen is a major component of structural tissues in the human body and accounts for more than 25% of the whole body protein content. Here, utilizing the current insights from biomineralization, we hypothesize that the binding affinity of nanoparticles to self-assembled collagen fibers is size and surface charge dependent.

*Experiments:* We developed a self-assembled collagen substrate compatible with Quartz Crystal Microbalance with Dissipation monitoring (QCM-D), which is very sensitive to mechanical changes of the substrate as a consequence of nanoparticle binding. QCM-D experiments were conducted with both positively and negatively charged gold nanoparticles between 2 and 10 nm in size. Complementary *ex situ* imaging Atomic Force Microscopy (AFM) and Scanning Electron Microscopy (SEM) were used to confirm the QCM-D results.

*Findings:* We find that both positively and negatively charged nanoparticles of all sizes exhibited binding affinity for self-assembled collagen fibers. Furthermore, the smallest particles (2 nm) mechanically integrated with collagen fibers.

Published by Elsevier Inc.

## 1. Introduction

Collagen is the principal protein component of many tissues including bone, connective tissue and skin and provides critical support to their exceptional mechanical properties [1,2]. Collagen self-assembles to form fibers (hundreds of nanometers in diameter) with 67 nm repeating band structures consisting of less dense gap and more dense overlap regions [3]. Recent results suggest that during the biological mineralization process, the interior of collagen fibers is infiltrated by nanometer sized amorphous calcium phosphate clusters [4,5], which ultimately crystallize to form the mineral apatite. These calcium phosphate clusters are characterized by (1) their small size, generally less than 10 nm, (2) their negative surface charge, [4] and (3) their fluid like character commonly referred to as the Polymer Induced Liquid Precursor (PILP) [6]. Due to the abundance of collagen in the human body, the nature of nanoparticle interactions with collagen fibrils is of fundamental interest in at least two perspectives: (1) biomimetic materials synthesis: how do CaP nanoparticles bind to and integrate with collagen fibers? And (2) toxicology: how do nanoparticles interact with matrix biomolecules?

Here, we hypothesize that in the first step to biomineralization, the interaction between nanoparticles (NP) with self-assembled collagen fibers is driven by the charge of the NP. We further test NP size dependent association with collagen. We developed a model system with gold nanoparticles (AuNP), which are chemically and colloidally stable to study the nature of collagen–AuNP interaction (amount, spatial distribution and reversibility) as a function of particle size and surface charge polarity. Here, we use AuNP ranging from 2 nm to 10 nm in size and possessing positive or negative charges. To study the nanoparticle/collagen binding process, we used Quartz Crystal Microbalance with Dissipation monitoring (QCM-D) along with Scanning Electron Microscopy (SEM) and Atomic Force Microscopy (AFM). QCM-D has been used extensively to quantify binding and subsequent conformation changes of proteins [7,8], other macromolecules [9], nanoparticles

*Abbreviations:* QCM-D, Quartz Crystal Microbalance with Dissipation monitoring; AFM, Atomic Force Microscopy; SEM, Scanning Electron Microscopy; AuNP, gold nanoparticle; $\Delta f$, frequency change; $\Delta D$, dissipation change; SD, Standard Deviation.

* Corresponding author.
*E-mail address:* slgibson@nist.gov (S. Lin-Gibson).

0021-9797/$ - see front matter Published by Elsevier Inc.
http://dx.doi.org/10.1016/j.jcis.2013.11.019

Author's personal copy



[10] binding to surfaces, as well as mineralization processes at surfaces [11].

The findings of this study have potential applications in nanoparticle toxicology, where understanding the fate of nanoparticles in the body after exposure is important [12]. Because of the prevalence of collagen as a structural protein throughout the body, understanding the role of nanoparticle size and charge governed interaction with collagen is essential.

## 2. Experimental

### 2.1. Preparation of QCM-D sensors

To clean the gold-coated QCM-D sensors (QSX-301, Biolin Scientific) they were exposed to Ultraviolet Ozone (UVO, Jelight) for 10 min; soaked in a solution composed of Deionized Water (DI) water (Milli-Q), hydrogen peroxide (30%, Fisher Scientific) and ammonium hydroxide (Sigma–Aldrich), at a proportion of 5:1:1, respectively, at 70 °C for 5 min, $N_2$ dried and finally exposed to UVO for 10 min. Afterward, the QSX-301 sensors were made hydrophobic by exposure to 1 mmol/L dodecane thiol (Sigma–Aldrich) dissolved in anhydrous alcohol (Warner-Grantham), rinsed with DI water then anhydrous ethanol and stored in anhydrous ethanol.

### 2.2. Preparation of collagen films

Dilute neutralized collagen solutions were prepared by first, mixing acidified type I collagen solution (pureCol, Advanced Biomedicals, 3 mg/mL) with 10X phosphate buffered saline (PBS) (Gibco) and 0.1 mol/L NaOH, at proportions of 8:1:1, respectively, with the final pH of approximately 7.4. Then the solution was diluted to a ratio of 1:7, neutralized collagen solution to 1X PBS [13]. Hydrophobically-modified QSX-301 sensors were immersed in diluted neutralized collagen solutions for 12–16 h at 37 °C. The collagen functionalized QSX-301 sensors were rinsed in 1X PBS and DI water and stored in 1X PBS at 4 °C until used.

### 2.3. Nanoparticle solutions

All nanoparticles solutions were diluted, if necessary, with DI water to 0.001% by mass $AuCl_4$ and then adjusted to pH 7.4 with 0.01 mol/L NaOH. Where Au concentration of the as received nanoparticle solutions are reported by the manufactures as mass% of the $AuCl_4$ reactant prior to reduction. Citrate stabilized gold nanoparticles (2 nm, 0.001% by mass $AuCl_4$; 5 nm, 0.01% by mass $AuCl_4$; and 10 nm, 0.01% by mass $AuCl_4$; all from British Biosciences) and an amine terminated polyethylene glycol stabilized gold nanoparticle (3 nm, 0.05% by mass $AuCl_4$, nanoOCS) were used.

### 2.4. QCM-D

Measurements were performed using a single flow module on the Q-Sense E4 experimental platform, operating at 25 °C with a peristaltic pump at 20 μL/min under continuous flow. Prior to nanoparticle introduction, collagen films were equilibrated in flowing DI water for 2 h. To assure the collagen film successfully formed on the surface the stitched QCM-D data from the baseline before collagen attachment (sensor plus DDT) and after collagen attachment showed a significant change (≈900 Hz in frequency ($\Delta f$) and ≈200 in Dissipation factor ($\Delta D$)). A baseline in flowing DI water was collected for ≈10 min prior to introduction of nanoparticle solutions (0.001% by mass $AuCl_4$). Collagen matrices were exposed to AuNP for 200 min and rinsed with DI water for 60 min. Changes in frequency ($\Delta f$) and Dissipation ($\Delta D$) were recorded for the fundamental frequency ($f$ = 5 mHz) and five overtones (3, 5, 7, 9 and 11 at 15 mHz, 25 mHz, 35 mHz, 45 mHz and 55 mHz). Each condition was repeated at least three times. Analysis of QCM-D data was performed with the QTools data analysis software. Data was fit using a one-layer Voigt model, with the following parameters: film density (1.36 g/cm$^3$ [14]), water density (1 g/cm$^3$) and fluid viscosity (1 mPa s) and using four overtones (3, 5, 7, 9). The following parameters were fit: film thickness, shear modulus and viscosity.

### 2.5. Preparation of $N_2$ dried samples

QCM-D sensors after exposure to AuNP were dried under a nitrogen stream for 1 min and then stored in a dry environment until imaging.

### 2.6. Preparation of critical point dried samples

QCM-D sensors after exposure to AuNP were removed from the flow module in a hydrated state, placed in DI water, incubated in ethanol/DI water mixtures of 10%, 25%, 50%, 75% then 100% ethanol for 10 min each and then placed into a critical point dryer (Tousimis Autosamdri – 814). Samples were stored in a dry environment until imaging.

### 2.7. Atomic Force Microscopy (AFM)

AFM images were collected on a Bruker Dimension Icon in Quantitative Nanomechanical Mapping (QNM) mode. All images were collected with a Tap150 probe (Bruker Inc.) ($k$ = 4 N/m, 8 nm nominal tip radius). At least 10 images were collected per condition and images presented are characteristic of each sample.

### 2.8. Scanning Electron Microscopy (SEM)

FEI Helios 650 Focused Ion Beam (FIB) SEM was used to collect SEM images. All images were collected at 1 kV, 50 pA electron beam condition with 1 mm working distance using a through-the-lens detector in backscatter mode. The images presented are characteristic of each sample, at least 10 images were collected per condition.

## 3. Results and discussion

AFM was used to characterize self-assembled collagen fibers on functionalized gold QCM-D sensors, which exhibited a bimodal distribution of fiber diameters of approximately 15 nm and approximately 100 nm (Fig. S1). The smaller fibers formed a dense mat on the surface of the QCM-D sensor, with larger fibers overlying these structures at a lower areal density, consistent with previous findings [13,15]. The larger fibers are more characteristic of hierarchically assembled type I collagen fibrils *in vitro* [4,5,16,17] and of collagen fibers found in tissue [18–21].

QCM-D was used to monitor changes of mechanical properties for self-assembled collagen as a result of interaction with AuNP. Generally, changes in frequency ($\Delta f$) are qualitatively related to mass change in the system, either adsorption (negative shift) or desorption (positive shift) [7]. Conversely, changes in Dissipation factor ($\Delta D$) are qualitatively related to mechanical properties of the system becoming more stiff (decrease) or more viscous (increase). Three replicate experiments were conducted for each condition. Between the replicate experiments the trends in changes of $\Delta f$ and $\Delta D$ were reproducible, although some variation in the maximum values $\Delta f$ and $\Delta D$ was observed (Table 1). Negatively charged (2 nm, 5 nm and 10 nm) and positively charged

Author's personal copy



**Table 1**
Comparison of the maximum values for change in frequency and dissipation during nanoparticle interaction for three replicates per condition. The reported errors represent 1 SD.

| Particle size (nm) | Charge polarity | $\Delta f_3$ (Hz) | $\Delta D_3$ | $\Delta f_5$ (Hz) | $\Delta D_5$ |
|---|---|---|---|---|---|
| 10 | – | −122 ± 13.2 | 6.4 ± 2.8 | −90.6 ± 9.2 | 23.5 ± 6.3 |
| 5 | – | −138 ± 23.9 | 13.8 ± 1.9 | −111 ± 25.7 | 26.1 ± 4.5 |
| 3 | + | −103 ± 12.9 | 11.3 ± 2.7 | −86.4 ± 10.4 | 19.2 ± 5.0 |
| 2 | – | 21 ± 22.0 | −90.4 ± 27.2 | −69.7 ± 54.6 | −60.2 ± 22.2 |

(3 nm) AuNP were used. Before experiments were conducted on self-assembled collagen, control experiments were carried out on dodecane coated sensor with each particle to ensure minimal interaction between NPs and sensor surface (Fig. S2). When collagen was exposed to AuNP with a diameter of 3 nm and larger, a negative frequency change ($\Delta f$) was observed, irrespective of charge polarity indicating particle binding to the collagen film (Fig. 1A–C). The corresponding increase in dissipation change ($\Delta D$) suggested that the nanoparticle binding caused the collagen/nanoparticle system to behave more viscous. The ability of collagen to interact with either positively or negatively charged species is not surprising because collagen possesses many charged moieties that are expected to interact with particles with either polarity [3,4,22]. The 2 nm particles caused the collagen/nanoparticle matrix to respond differently as compared to the larger particles. Interactions between 2 nm particles and collagen caused an initial negative shift in $\Delta f$, which was quickly followed by a positive shift in the 3rd overtone. A negative $\Delta f$ shift in the higher overtones (5th and 7th) was observed but at a lower magnitude as compared to the larger particles. Contrary to the adsorption of larger AuNP, the addition of 2 nm AuNP caused a decrease in $\Delta D$ indicating that the nanoparticle binding caused the collagen/nanoparticle matrix to become more rigid.

The difference in AuNP/collagen interaction between the 2 nm particles and larger particles was further substantiated from $\Delta D$ vs. $\Delta f$ plots of the 5th overtone. The amount of dissipation per unit frequency change ($\Delta D/\Delta f$ ratio) provided a visualization of viscoelastic change as a function of mass change without time as an explicit parameter [9,23]. Fig. 2 indicates that the adsorption of larger AuNP to collagen resulted in a similar viscoelastic response, in which a decrease in $\Delta f$ (more mass) is correlated with an increase in $\Delta D$ (more viscous). The 2 nm adsorption was characterized by two discrete regimes. At low $\Delta f$ (lower nanoparticle density in the system) the behavior of the collagen matrix was indistinguishable from those of the larger nanoparticles. At higher $\Delta f$ (higher nanoparticle density in the system), a decrease in dissipation occurs. This drop caused a negative slope in the $\Delta D$ vs. $\Delta f$ plot, suggesting a change in the mechanical behavior of the collagen/nanoparticle matrix. The inflection in the $\Delta D/\Delta f$ curve suggested a particle density dependent phenomenon. At low particle densities, the system behaved similarly to the larger nanoparticle systems. However, at larger $\Delta f$ (higher particle densities), the ensemble matrix (collagen plus nanoparticles) experienced a decrease in $\Delta D$, indicating an increase in rigidity. The sudden onset of rigidity in the collagen/nanoparticle system may represent a percolation threshold: the particle density dependent formation

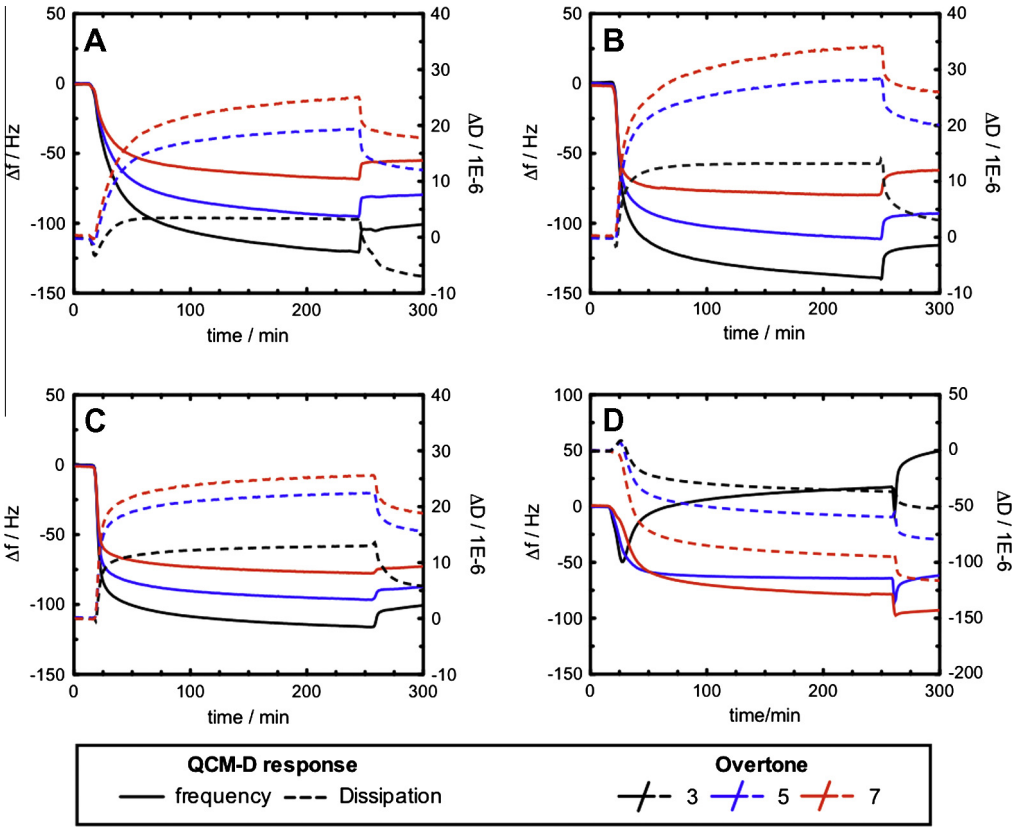


**Fig. 1.** Representative QCM-D data of gold nanoparticle (AuNP) interactions with collagen: $\Delta f$ (solid lines) and $\Delta D$ (dashed lines) for (A) 10 nm citrate stabilized AuNP, (B) 5 nm citrate stabilized AuNP, (C) 3 nm amine/PEG stabilized AuNP, and (D) 2 nm citrate stabilized AuNP. Introduction of nanoparticles is at ≈25 min, and DI rinse solution is introduced at ≈250 min.

Author's personal copy



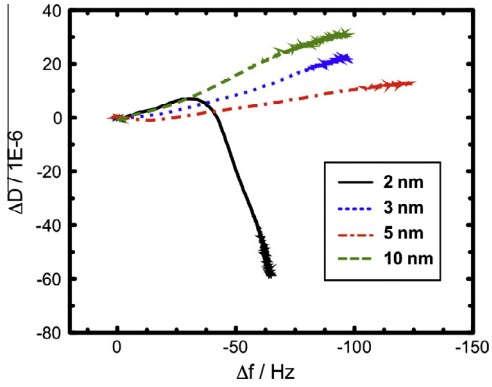


**Fig. 2.** Representative $\Delta D$ vs. $\Delta f$ behavior of the 5th overtone. The behavior of the larger nanoparticles is typical of a viscoelastic response. At low $\Delta f$, the 2 nm system follows the same behavior, however at higher $\Delta f$ the response changes.

of an extended and interconnected network of nanoparticles [24]. Similar particle density dependent phenomenon has been reported for Ag precipitation in skin collagen fibers [25], where a critical particle density is associated with a sudden and significant increase in conductivity.

To further substantiate the interpretations, QCM-D data were fit using a single layer Voigt model (Fig. S3, data along with fit Fig. S4). Qualitatively, the Voigt model indicates deposition of larger particles causes an increase in film thickness (or mass) and slight increases in viscosity and shear modulus. This behavior is consistent with classical biomolecule/surface adsorption behavior [9]. However, the case for the deposition of the 2 nm particles is significantly different. Especially, the positive shift in $\Delta f$ for the 3rd overtone is somewhat surprising; generally, in simple systems, when such behavior is observed it is due to the loss of mass that is mechanically coupled to the sensor, which is likely not the case. All the higher overtones show a negative shift in $\Delta f$, indicating mass increase, which is consistent with nanoparticle deposition. In this case, the changes in $\Delta f$ are captured by the Voigt model (Fig. S4D), which indicates a decrease in film thickness and a slight increase in viscosity along with a significant increase in shear modulus upon the deposition of the 2 nm AuNP. These modeling results, while qualitative, did indicate that 2 nm particles mechanically integrate with collagen fibers, differing from the larger nanoparticles, which likely only adsorb to the surface.

The strength of the AuNP–collagen interaction was assessed by a rinsing process in the QCM-D [9] (Fig. 1, after 250 min). Loosely bound AuNP are expected to completely or partially dissociate from the surface whereas tightly bound AuNP are expected to remain attached to the collagen. Upon rinsing, $\Delta f$ increased and $\Delta D$ decreased for larger AuNP, although not fully recovering to the original values. These results indicated a fraction of AuNP was removed from the collagen, but some particles remained attached. This type of behavior with collagen has been observed with CdSe nanoparticles as well as BSA conjugated Au nanoparticle [26,27] and is also in contrast to previous reports of CdSe nanoparticles on self-assembled monolayers of functionalized alkane thiols where on a simple model charged organic surface the nanoparticle adsorption process is completely reversible [10]. The 2 nm nanoparticles exhibited different frequency and dissipation behaviors. $\Delta f$ remained unchanged or increased, indicating few, if any, nanoparticles dissociated from the collagen/nanoparticle matrix. Additionally, $\Delta D$ decreased similar to the other particles; however, a decrease indicated a larger deviation from the original collagen only matrix in DI water. Such response corresponded to a lack of AuNP removal and further stiffening of the collagen/nanoparticle film.

SEM and AFM images of collagen matrices after QCM-D experiments were collected to evaluate the spatial distribution of AuNP. Note that the samples were prepared differently to maximize contrast in different imaging modalities. Critical point dried (CPD) samples revealed significantly better contrast by SEM for nanoparticles and collagen (compare Fig. S5 with Fig. 3A) and $N_2$ dried samples produced significantly better contrast for collagen by AFM adhesion mode (compare Fig. 3G with Fig. S5). Additionally, different sample preparation techniques preserved different aspects of collagen film morphology. Specifically, CPD samples better preserved (as compared to $N_2$ dried samples) hydrated

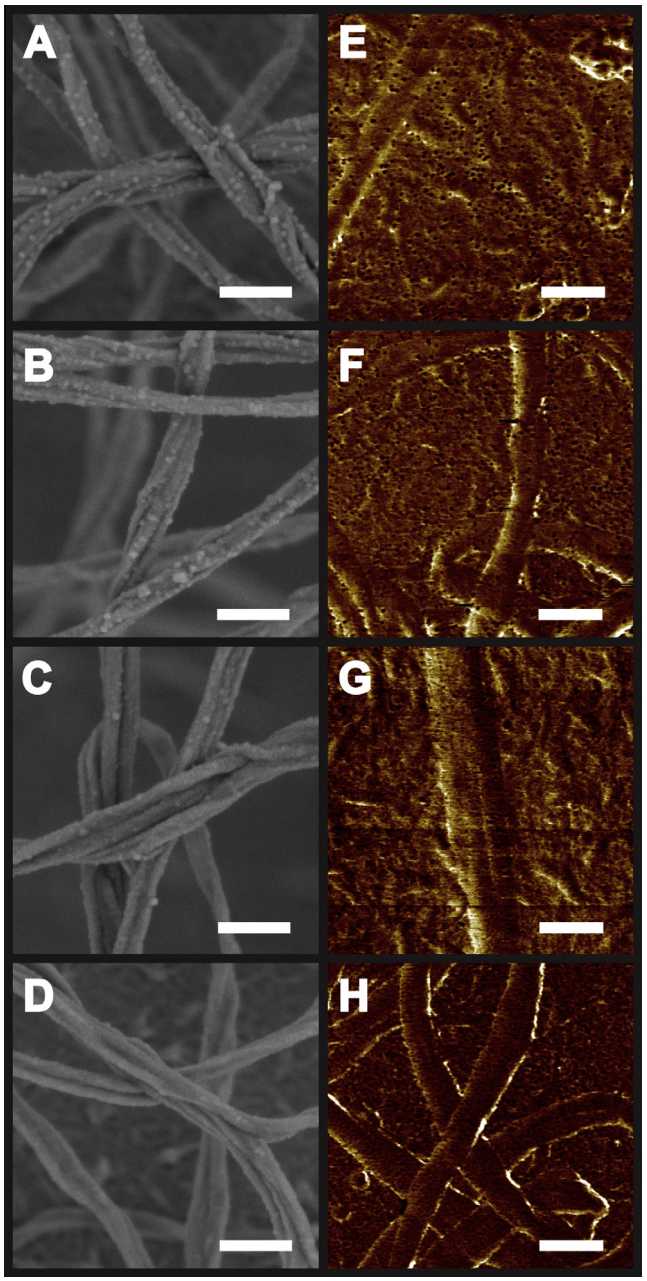


**Fig. 3.** (A–D) SEM images of critical point dried, mineralized collagen. (E–H) AFM adhesion mode images of $N_2$ dried, mineralized collagen samples. In SEM images, light regions correspond to gold nanoparticles. In AFM adhesion mode images, dark regions correspond to gold nanoparticles. (A and E) are images of 10 nm citrate stabilized gold nanoparticles. (B and F) are images of 5 nm citrate stabilized gold nanoparticles. (C and G) are images of 3 nm amine/PEG stabilized gold nanoparticles. (D and H) are images of 2 nm citrate stabilized gold nanoparticles. Scale bars = 200 nm.

Author's personal copy



morphologies of the collagen and in the SEM images AuNP appear bright from high Z contrast (Fig. 3A–D). $N_2$ dried samples produced collapsed collagen structures (height ≈ 10 nm), and AuNP appear as dark features in AFM adhesion mode, indicating regions of low tip/surface adhesion (Fig. 3E–G) [28]. Both SEM and AFM images clearly showed the presence of particles on the surface of collagen for the 3 nm, 5 nm and 10 nm nanoparticles (Fig. 3A–C, E–G). Additionally, SEM images showed that the particles are located on the periphery the collagen fibers for larger particles. AFM images (Fig. 3E–G) showed uniform nanoparticle distribution across the surface and no nanoparticle preference for small or large collagen fibers. These results indicate collagen–AuNP is nonspecific, e.g. no preferential interaction between AuNP and the gap regions (lower density regions) of the collagen fibrils with 67 nm repeats. This is in contrast with CaP clusters in biomimetic mineralization, which are generally believed to enter the fibrils in the gap regions of the collagen fibril [4].

AFM images revealed that the 2 nm particles on collagen were clearly visible when prepared by $N_2$ drying (Fig. 3H) as particles homogeneously distributed throughout the surface of the collagen film. In similar CPD samples nanoparticles, were only faintly detected by SEM (Fig. 3D) and not detectable by AFM adhesion mode images (Fig. S6B). The clear ability to detect nanoparticles in collapsed collagen structures and inability to detect nanoparticles in uncollapsed collagen structures, may suggest that the particles are slightly buried within the collagen fibers, consistent with QCM-D data showing that the 2 nm particles mechanically integrate with the collagen fibrils.

In biomineralization, the critical first step to collagen mineralization is the binding of CaP particles to collagen. Our QCM-D and microscopy data indicate for nanoparticles to bind with collagen, the overall charge can be positive or negative. The second step is for CaP clusters to infiltrate into the interior of collagen fibers. Our results indicate that penetration into collagen fibers is not likely for rigid particles larger than 3 nm. We note that larger CaP clusters (>10 nm) have to been shown to infiltrate into collagen fibers [4]. The difference in the size limit between AuNP and CaP clusters may be explained by the liquid-like properties attributed to CaP clusters [6], allowing them to access the interior of collagen fibrils. As noted earlier, AuNP did not form specific interaction with collagen structures, whereas CaP clusters likely infiltrate collagen fibrils preferentially through the gap regions.

These results suggest that in low ionic strength conditions where citrate stabilized gold nanoparticles are colloidally stable, charged nanoparticles are highly attracted to collagen. These results inspired by the biomineralization may have important implications for understanding the toxicity of nanoparticles, where affinity of nanoparticles and proteins are of critical importance [12]. We acknowledge this study explores a narrow range of low ionic strengths of simple electrostatically stabilized nanoparticles to understand their size and charge dependent affinity to collagen. However, this type of approach may be broadly applicable in more physiologically relevant solutions as long as the nanoparticles of interest remain well dispersed. The advantage of such a QCM-D based approach is that screening different conditions can be relatively high throughput and in this type of relatively well-constrained system, nanoparticles that have high affinity to collagen can be quickly and easily detected.

## 4. Conclusions

We have developed a QCM-D based approach for investigating nanoparticle binding to self-assembled collagen fibers, a model for structural proteins. It was demonstrated that nanoparticles of both negative and positive charge polarities have affinity for collagen fibers. The smallest tested 2 nm particles produced a stiffening response in the system that is sudden and particle density dependent, suggesting a percolation threshold. Additionally, imaging data demonstrates that nanoparticle binding to collagen fibers is not spatially specific, unlike biomimetic mineralization where calcium phosphate nanoparticles interact with gap regions in collagen fibers.

## Funding sources

This work is in part supported by an Interagency Agreement Y1-DE-7005-01 between the National Institute of Standards and Technology (NIST) and the National Institute of Dental and Craniofacial Research (NIDCR).

## Notes

Official contribution of NIST; not subject to copyrights in USA. Certain commercial materials and equipment are identified in this article to specify the experimental procedure. In no instance does such identification imply recommendation or endorsement by NIST or that the material or equipment identified is necessarily the best available for the purpose.

## Acknowledgments

D.W. acknowledges the NIST-NRC Research Associate Program for support. We thank N.J. Lin for helpful discussions and comments.

## Appendix A. Supplementary material

Supplementary data associated with this article can be found, in the online version, at http://dx.doi.org/10.1016/j.jcis.2013.11.019.

## References

[1] K.J. Koester, J.W. Ager, R.O. Ritchie, Nat. Mater. 7 (2008) 672.
[2] X. Wang, R.A. Bank, J.M. Tekoppele, C.M. Agrawal, J. Orthopaed. Res. 19 (2001) 1021.
[3] J.P.R.O. Orgel, T.C. Irving, A. Miller, T.J. Wess, Proc. Natl. Acad. Sci. 103 (2006) 9001.
[4] F. Nudelman, K. Pieterse, A. George, P.H.H. Bomans, H. Friedrich, L.J. Brylka, P.A.J. Hilbers, G. de With, N.A.J.M. Sommerdijk, Nat. Mater. 9 (2010) 1004.
[5] Y. Liu, Y.-K. Kim, L. Dai, N. Li, S.O. Khan, D.H. Pashley, F.R. Tay, Biomaterials 32 (2011) 1291.
[6] T.T. Thula, F. Svedlund, D.E. Rodriguez, J. Podschun, L. Pendi, L.B. Gower, Polymers 3 (2011) 10.
[7] A.R. Patel, K.K. Kanazawa, C.W. Frank, Anal. Chem. 81 (2009) 6021.
[8] E. Gurdak, C.C. Dupont-Gillain, J. Booth, C.J. Roberts, P.G. Rouxhet, Langmuir 21 (2005) 10684.
[9] K.D. Kwon, H. Green, P. Bjöörn, J.D. Kubicki, Environ. Sci. Technol. 40 (2006) 7739.
[10] J.J. Park, S.H.D.P. Lacerda, S.K. Stanley, B.M. Vogel, S. Kim, J.F. Douglas, D. Raghavan, A. Karim, Langmuir 25 (2008) 443.
[11] S.C. Ngourn, H.A. Butts, A.R. Petty, J.E. Anderson, A.E. Gerdon, Langmuir 28 (2012) 12151.
[12] A. Alkilany, C. Murphy, J. Nanopart. Res. 12 (2010) 2313.
[13] J.T. Elliott, J.T. Woodward, A. Umarji, Y. Mei, A. Tona, Biomaterials 28 (2007) 576.
[14] A. Peterson, M. Halter, A. Tona, K. Bhadriraju, A. Plant, BMC Cell Biol. 10 (2009) 16.
[15] K.-H. Chung, K. Bhadriraju, T.A. Spurlin, R.F. Cook, A.L. Plant, Langmuir 26 (2010) 3629.
[16] A.S. Deshpande, E. Beniash, Cryst. Growth Des. 8 (2008) 3084.
[17] F. Jiang, H. Hörber, J. Howard, D.J. Müller, J. Struct. Biol. 148 (2004) 268.
[18] V. Jantou, M. Turmaine, G.D. West, M.A. Horton, D.W. McComb, Micron 40 (2009) 495.
[19] V. Jantou-Morris, M.A. Horton, D.W. McComb, Biomaterials 31 (2010) 5275.
[20] E.A. McNally, H.P. Schwarcz, G.A. Botton, A.L. Arsenault, PLoS One 7 (2012) e29258.
[21] J.M. Wallace, Q.S. Chen, M. Fang, B. Erickson, B.G. Orr, M.M.B. Holl, Langmuir 26 (2010) 7349.

Author's personal copy



[22] B. Cantaert, Y.-Y. Kim, H. Ludwig, F. Nudelman, N.A.J.M. Sommerdijk, F.C. Meldrum, Adv. Funct. Mater. 22 (2012) 907.
[23] F. Höök, M. Rodahl, B. Kasemo, P. Brzezinski, Proc. Natl. Acad. Sci. 95 (1998) 12271.
[24] S.B. Kharchenko, J.F. Douglas, J. Obrzut, E.A. Grulke, K.B. Migler, Nat. Mater. 3 (2004) 564.
[25] J. Guo, X. Wang, X. Liao, W. Zhanga, B. Shi, J. Phys. Chem. C (2012).
[26] J.J. Park, M.C. Weiger, S.H. De Paoli Lacerda, D. Pristinski, M.L. Becker, J.F. Douglas, D. Raghavan, A. Karim, Langmuir 26 (2010) 4822.
[27] C. Bhan, R. Mandlewala, A. Gebregeorgis, D. Raghavan, Langmuir 28 (2012) 17043.
[28] A. Pakzad, J. Simonsen, R.S. Yassar, Compos. Sci. Technol. 72 (2012) 314.